NONLINEAR ELASTIC TOMOGRAPHY USING SPARSE ARRAY MEASUREMENTS

Francesco Ciampa[1], Simon Pickering[1], Gennaro Scarselli[2], Andrea Giampiccolo[1], Michele Meo[1]

[1] *Material Research Centre, Department of Mechanical Engineering, University of Bath, Bath, BA2 7AY, UK*
[2] *Dipartimento di Ingegneria dell'Innovazione, Università del Salento, Via per Monteroni, Lecce, Italy*

f.ciampa@bath.ac.uk

ABSTRACT

Literature offers a quantitative number of diagnostic imaging methods that can continuously provide a detailed image of the material defects in aerospace and civil applications. This paper presents a nonlinear Structural Health Monitoring (SHM) imaging method, based on nonlinear elastic wave tomography (NEWT), for the detection of the nonlinear signature in damaged isotropic structures. The proposed technique, based on a combination of higher order statistics (HOS) and radial basis function (RBF) interpolation, is applied to a number of waveforms containing the nonlinear responses of the medium. HOS such as bispectral analysis and bicoherence was used to characterize the second order nonlinearity of the structure due to corrosion, whilst RBF interpolation was applied to a number of signals acquired from a sparse array of sensors, in order to obtain an image of the defect. Compared to standard linear ultrasonic imaging techniques, the robustness of this nonlinear tomography sensing system was experimentally demonstrated. Moreover, this methodology does not require any baseline with the undamaged structure for the detection of the nonlinear source as well as a priori knowledge of the mechanical properties of the medium. Finally, the use of HOS makes NEWT a valid alternative to traditional nonlinear elastic wave spectroscopy (NEWS) methods for materials showing either classical or non-classical nonlinear behaviour.

KEYWORDS: *nonlinear elastic tomography, damage detection, imaging method, SHM applications.*

INTRODUCTION

Damage detection is getting more and more attention from scientists and engineers operating in the aerospace field since composite materials have become a structural material adopted for aircraft primary structures (wing, fuselage) of large airliners and not only for secondary structural elements. Non Destructive Techniques play a major role in qualification of process and products and ensure that structural components do not have internal or surface defects. Nevertheless, the attention of scientific community is focused on acousto/ultrasonic Structural Health Monitoring (SHM) imaging techniques, based on guided waves (GW), which are able to identify and localise damages in operating conditions before these could lead to catastrophic failures [1]. There are different ultrasonic GW imaging methods that can be adopted for SHM falling in two big categories, i.e. linear and nonlinear. The former ones require a baseline whilst the latter do not. A baseline should represent the structural behaviour of the undamaged sample and it can correspond to operational mode shapes, natural frequencies, vibrational and acoustic signals properly chosen. The effect of damage on the natural frequencies of a sample has been investigated as a potential global inspection technique, but this approach has been proved to be sensitive to environmental factors [2]. Other

linear methods have been proved to be more effective in damage localisation: among these, tomography [3], time-of-arrival [4], time-difference-of-arrival [5], energy arrival [6] and Reconstruction Algorithm for the Probabilistic Inspection Damage (RAPID) method [7]. All these methods are based upon the signals between pairs of N transducers, i.e. they post-process the differences between signals acquired for the undamaged and the damaged structure in different locations and build several figures of merit allowing the prediction of the damage location. Rayleigh Maximum Likelihood Estimation (RMLE) method is another linear technique able to locate structural damage using guided waves to feed a Rayleigh based statistical model of scattered wave measurements [8]. However, the large changes in nonlinear ultrasonic parameters for small degrees of damage have stimulated interest in the use of nonlinearity for fatigue crack detection: nonlinear elastic wave spectroscopy (NEWS) shows promise as a route to a sensitive crack detection method [9], [10]. In Kyung-Young [11], the use of nonlinear ultrasonic waves for evaluation of material degradation was presented. The generation mechanism of the second-order harmonic frequency components during the propagation of elastic stress waves through the degraded material was first explained on the basis of nonlinear elasticity. Then, higher order statistics (HOS) analysis was used for the measurement of the nonlinear parameter β, indicating the ratio of the amplitude of second-order harmonic frequency components relative to the power of the fundamental. Finally, several experiments were carried out to confirm the correlation between the second order nonlinear parameter β and the material degradation. The results showed that β is proportional to the magnitude of the load and the number of fatigue cycles and well reflected the actual variation of the specimen strength. In Ciampa et al. [12], nonlinear elastic wave tomography (NEWT) was used as a useful diagnostic tool to image the presence of a crack or defect in composite structures. The bispectrum signal processing technique was employed to analyse the nonlinear response of the sample undergone to harmonic continuous excitation. Particularly, a bispectral matrix was generated allowing the definition of a damage map overlapping the sample formed by discrete values of bispectrum. The results showed a strong correlation of the parameter β and bicoherence with damage in the sample and encouraged the use of nonlinear ultrasonic as structural health monitoring (SHM) imaging technique. In the present paper the different imaging methods of damage detection before mentioned, i.e. linear and nonlinear, are applied to detect and localise the damage on a typical aluminium panel for aerospace applications undergone to pitting corrosion. Initially a baseline was obtained for the undamaged structure, then a controlled material degradation process was activated over a small region of the panel surface and the effect of this induced damage was evaluated. A comparison of the different techniques in providing reliable prediction on this simple structure was performed allowing useful discussion about the suitability of each of them. The layout of this paper is as follows: in Section 1, the different linear methods are briefly presented and discussed. Section 2 illustrates nonlinear methods. Section 3 illustrates the experimental set-up, whilst Section 4 reports the results provided by the different techniques. Finally, conclusions are drawn and summarised.

1 LINEAR METHODS

Hilbert Transformation

If $s_{ij}(t)$ is the signal recorded from each pair (baseline) with no damage, $f_{ij}(t)$ is the signal recorded from each pair with damage. The residual signal is:

$$r_{ij}(t) = f_{ij}(t) - s_{ij}(t) \tag{1}$$

The complex analytical signal is formed from this signal and its Hilbert transform $c_{ij}(t)$:

$$c_{ij}(t) = r_{ij}(t) + iv_{ij}(t) \tag{2}$$

The envelope detected residual signal is:

$$h_{ij}(t) = \sqrt{r_{ij}(t)^2 + v_{ij}(t)^2} \tag{3}$$

Time-Of-Arrival (TOA) (or Ellipse) Algorithm

If (x_i, y_i) is the transmitter (*tr*) position, (x_j, y_j) is the receiver (*rec*) and (x, y) any point (*p*) of the structure, the time that the signal takes to travel from the transmitter location to the any point of the panel and the receiver is [4]:

$$t_{ij}(x,y) = \frac{d_{tr-p}}{c_g} + \frac{d_{rec-p}}{c_g} = \frac{\sqrt{(x_i - x)^2 + (y_i - y)^2}}{c_g} + \frac{\sqrt{(x_j - x)^2 + (y_j - y)^2}}{c_g} \tag{4}$$

By calculating $h_{ij}(t_{ij}(x,y))$, a spatial map of the subtracted signals is obtained. Therefore, for all transducers pairs combination in the array, the final amplitude map is:

$$I_{TOA}(x,y) = \frac{1}{N_p} \sum_{i=1}^{N-1} \sum_{j=i+1}^{N} h_{ij}(t_{ij}(x,y)) \tag{5}$$

where N is the number of sensors in the array and $N_p = \frac{N(N-1)}{2}$. Equation (5) means that values of the amplitude obtained at certain time (i.e. at the coordinate x and y) were first added for each pair and then averaged. For a single transducer pair, this imaging algorithm maps a single echo to an ellipse with its foci being the transmitter-receiver location. As additional pairs are added, the ellipses intersect at defect location and thus reinforce.

Time-Difference-Of-Arrival (TDOA) (or Hyperbola) algorithm

This algorithm [5] is based on the assumption that the received waveform at two sensing transducer, as actuated by the same transmitting transducer, can be correlated according to the time difference in the Time-Of-Flight (TOF) from a given region to each of the receiver transducer. Assuming that a transmitter (x_n,y_n) send a signal, the time difference that the waveform would take to travel from the source to a given point (x,y) on the panel and on to each of the two locations of receiver (x_i,y_i) and (x_j,y_j) would be:

$$\begin{aligned} \Delta t_{ij} &= \left(\frac{d_{tr-p}}{c_g} + \frac{d_{i-p}}{c_g} \right) - \left(\frac{d_{tr-p}}{c_g} + \frac{d_{j-p}}{c_g} \right) = \frac{d_{i-p}}{c_g} - \frac{d_{j-p}}{c_g} = \\ &= \frac{\sqrt{(x_i - x)^2 + (y_i - y)^2}}{c_g} - \frac{\sqrt{(x_j - x)^2 + (y_j - y)^2}}{c_g} \end{aligned} \tag{6}$$

If $s_{in}(t)$ and $s_{jn}(t)$ are the signals recorded from the receivers i and j with no damage (baseline) and $f_{in}(t)$ and $f_{jn}(t)$ are the signals recorded from the receivers i and j with damage, the residuals are:

$$\begin{aligned} r_{in}(t) &= f_{in}(t) - s_{in}(t) \\ r_{jn}(t) &= f_{jn}(t) - s_{jn}(t) \end{aligned} \tag{7}$$

The time difference is calculated using the cross-correlation $R_{in,jn}(t)$ between the two residual signals. If a damage is present at the point (x_{d0}, y_{d0}), its reflections will appear in the two residual signals with different time delays, and the cross-correlation function will give a maximum value at $\Delta t_{ij}(x_{d0}, y_{d0})$. However, there are many combinations of points (x, y) of the structure which will give the same time delay $\Delta t_{ij}(x_{d0},y_{d0})$. Hence, a spatial map will be reproduced if the value $R_{in,jn}(t)$ are plotted for each point (x,y) at its corresponding time delay $\Delta t_{ij}(x_{d0},y_{d0})$. The intensity map is given by:

$$I_{TDOA}(x,y) = \sum_{n=1}^{N} \sum_{\substack{i=1 \\ i \neq n}}^{N-1} \sum_{\substack{j=i+1 \\ j \neq n}}^{N} R_{in,jn}(\Delta t_{ij}(x,y)) \tag{8}$$

The maximum correlation is a serious of hyperboles that cross the location of the defect with the foci on the two receivers.

Energy Arrival (EA) Method

This approach [6] is an adaptively windowed version of the TOA Algorithm, where the contribution of a component of a waveform is inversely weighted by the wave energy that arrived before it. The residual signal is $r_{ij}(t)$ for the transducer pair ij, and each of these signals can be windowed about the calculated arrival time for that transducer pair. The image is calculated according to:

$$I_{EA}(x,y) = \sum_{i=1}^{N-1} \sum_{j=i+1}^{N} \frac{E_{ij}^{win} - E_{ij}^{cum}}{E_{ij}^{win} + E_{ij}^{cum}} \tag{9}$$

where:

$$E_{ij}^{win} = \int_{t_{ij}}^{t_{ij}+\Delta t} r_{ij}^{\,2}(t)dt; \quad E_{ij}^{cum} = \int_{0}^{t_{ij}} r_{ij}^{\,2}(t)dt \tag{10}$$

Δt is the width of the time window, beginning at the calculated arrival time t_{ij}. The inversion of the wave energy adaptively reduces the amplitude of the scattered echoes.

RAPID (Reconstruction Algorithm for the Probabilistic Inspection Damage) algorithm
This method [7] defines on image over the sample subject of investigation through the following spatial distribution function:

$$I_{RAPID}(x,y) = \sum_{i=1}^{N-1} \sum_{j=i+1}^{N} SDC_{ij} s_{ij}(x,y) \tag{11}$$

where SDC_{ij} is a term associated to the covariance between the damaged and undamaged structural signals and $s_{ij}(x,y)$ is a purely geometric term.

Rayleigh Maximum Likelihood Estimator (RMLE)
This method [8] consists of finding the maximum of the Rayleigh likelihood function at the damage location:

$$\hat{\mathbf{x}} = \arg\max_{x,y} \left[I_{RMLE}(x,y) \right] \tag{12}$$

where $\mathbf{x}$ is the vector coordinates x and y on the structural surface.

2 NONLINEAR ELASTIC WAVE TOMOGRAPHY

According to Landau's nonlinear classical theory [13], the standard second order nonlinear parameter β can be obtained as a solution of the nonlinear elastodynamic wave equation via a first order perturbation theory as follows

$$\beta \propto \frac{\sqrt{|P(\omega_2)|}}{|P(\omega_1)|} \tag{13}$$

where $|P(\omega_2)|$ is the magnitude of the power spectral density associated with the second harmonic frequency component. The parameter β is able to quantify the second nonlinear elastic response of a structure subjected to sinusoidal excitation. An analogous nonlinear parameter can be obtained from higher order statistics in order to measure the amount of coupling between the angular frequencies ω_1 and $\omega_2=2\omega_1$. In particular, the bicoherence b^2 is a useful normalized form of bispectrum that measures Quadratic Phase Coupling on an absolute scale between 0 and 1 and can be defined as [14]:

$$b^2 = \frac{|B(\omega_1,\omega_1)|^2}{P(\omega_1)P(\omega_1)P(\omega_2)} \tag{14}$$

Since the bispectrum $B(\omega_1,\omega_2)$ has a variance proportional to the triple product of the power spectra, it can result in the second order properties of the acquired signal dominating the estimation. The advantage of normalisation is to make the variance approximately flat across all frequencies. Hence,

both the parameters β and the bicoherence b^2 will be used to characterise the nonlinearity of the structural response of the aluminium panel subjected to a harmonic excitation. Furthermore, according to [12], a radial basis function (RBF) approach was employed to create the nonlinear elastic wave tomography images $I_{\beta}(x,y)$ and $I_{b^2}(x,y)$ of the damage location using a sparse array or receivers sensors.

3 EXPERIMENTAL SETUP

The investigated structure was an aluminium panel with dimensions of 600 x 600 mm x 5 mm. Over the top panel surface eight piezoelectric sensors were surface bonded (see Fig. 1). Each sensor was used as transmitter while the others served as receivers allowing the realization of 8 matrices 7x7 then summed and post-processed. The transmitter sensor was linked to a preamplifier and connected to a National Instrument (NI) data acquisition system consisting of the NI PXI 5421 16-bit arbitrary waveform generator card to send an 80-cycles Hanning-windowed tone burst at 200 kHz. The excited voltage applied was around 150 V in order to maximize the efficiency of the available sensors. The plate was instrumented with eight, 10 mm circular piezoelectric tranducers designed to excite and measure the fundamental symmetric Lamb mode S_0. At the chosen excitation frequency, the wavelength of the propagating wave S_0 was around 25 mm. The undamaged structure was first tested for evaluating the baseline. Then, corrosion damage was introduced through a controlled material degradation process and finally imaging tests were performed.

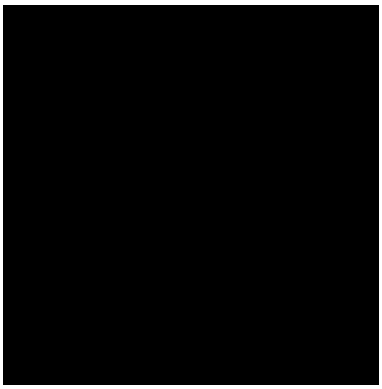

Figure 1: Sensors configuration and damage location.

3.1 The Corrosion Process

After the application of a Teflon mask, a surface of 10 x 10 mm was subjected to three different corrosion processes. The first process involved HNO_3 concentrated (Sigma-Aldrich 70%, density of 1,413 g/mL at 20 °C). A uniform layer of HNO_3 was deposited using a glass pipette [15]. After three hours, 2g of bicarbonate was used to neutralize the acid environment. The surface was cleaned with distilled water. A change of colour was noticed as a proof of the action of the acid on the first layer of aluminium oxide that naturally covers the surface of an aluminium alloy. The second process was mechanical and aimed to accelerate the corrosion action by the acids over the chosen surface. Particularly, a small notch was created with a chisel. The third process consisted of an attack with H_2SO_4 concentrated (Sigma-Aldrich, ACS reagent, 95.0-98.0%, density of 1,840 g/mL at 25 °C) according to Ghali [16]. An attack with H_2SO_4 is strong enough to corrode the surface enchanting a pitting corrosion following the notch made with the mechanical process.

4 RESULTS

The following figures report the results of the application of the different imaging methodologies for the damage localisation.

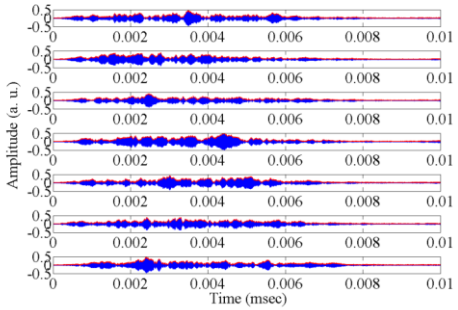

Figure 2: Residual signals.

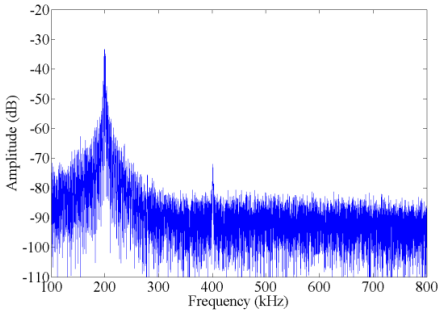

Figure 3: Spectrum of the measured signal.

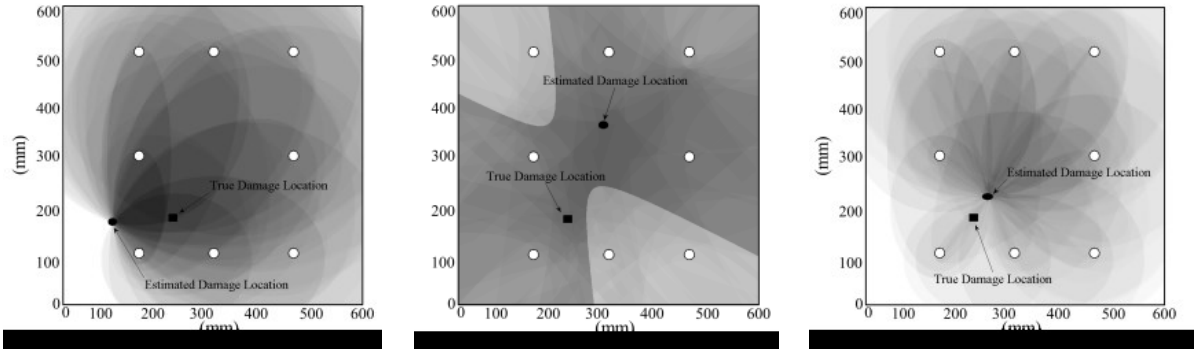

TOA TDOA EA

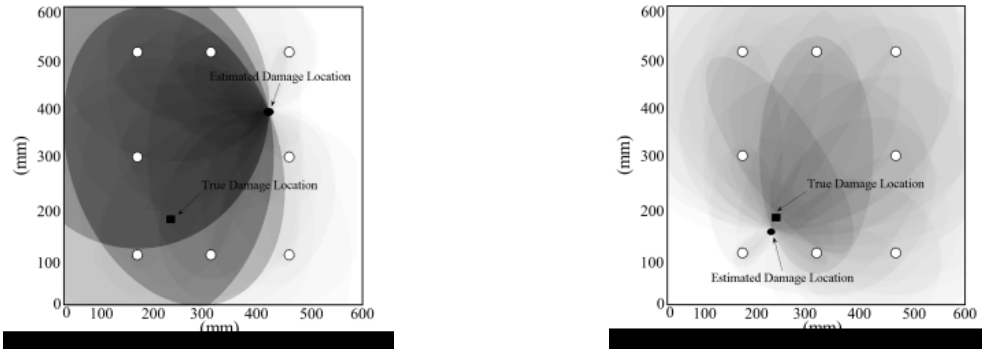

RAPID RMLE

Figure 4: Application of linear methods for the damage localization.

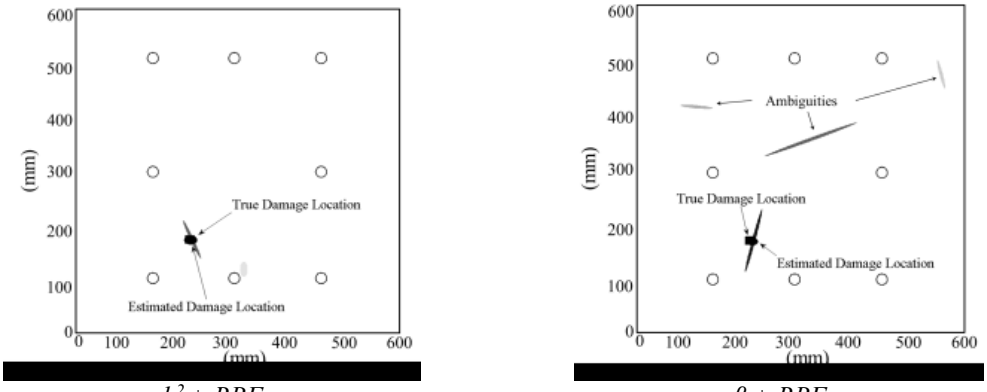

b^2 + *RBF* β + *RBF*

Figure 5: Application of nonlinear methods for the damage localization.

It is clear from the Figure 2 that there is a strong difference between the signals for the undamaged and damaged structure. The blue waveforms represent the acquired time histories, whilst the red ones are the associated envelopes. From Figure 3 it is evident the presence of a second harmonic at 400 kHz due to nonlinear interactions of the elastic wave with the damage. Predictive capability of the methods is measured on the post-processing of these residuals in order to find the exact location of the damage due to corrosion. Among linear imaging techniques, the most accurate prediction was achieved using RMLE technique. Indeed, according to Table 1 and the error function χ defined by $\chi = \sqrt{(x_d - x_{d0})^2 + (y_d - y_{d0})^2}$, where x_d and y_d and x_{d0} and y_{d0} are the coordinates of the estimated and true damage location, respectively, a maximum estimation error of $\chi = 25$ mm in the damage location was found using RMLE technique.

Table 1: Damage coordinates and error function for both linear and nonlinear imaging methods

	x-coordinate (mm)	y-coordinate (mm)	Error Function ψ (mm)
TOA – 8 Sensors	120	185	poor localisation
EA – 8 Sensors	270	225	40
TDOA – 8 Sensors	310	365	poor localisation
RAPID – 8 Sensors	430	400	poor localisation
RMLE – 8 Sensors	230	175	25
β + RBF – 8 Sensors	251	190	no error + ambiguities
b^2 + RBF – 8 Sensors	250	290	no error

Figure 5 showed that a combination of bicoherence analysis and radial basis function allowed a perfect localization of the pitting corrosion location with an error function equal to zero. However, unlike bicoherence, the nonlinear imaging with the standard second order nonlinear parameter β provided not only perfect damage localisation, but also ambiguities over the surface panel. This was due to the lack of information provided by the quadratic phase coupling between the fundamental and the second harmonic for the calculation of the second order nonlinear coefficient [12]. Indeed, the parameter β does not provide any information on the phase of the measured signals, which may lead to ambiguities in the image of the nonlinear source. Such ambiguities could be produced by spurious experimental sources of nonlinearity such as the amplifier and the excitation transducer due to the high input amplitude, or the coupling between the receiver sensor and the aluminium structure.

CONCLUSION

In the present paper an aluminium panel for aerospace applications has been tested for comparing a nonlinear SHM imaging method, based on nonlinear elastic wave tomography (NEWT), with different linear damage detection techniques. The linear techniques indeed require a baseline of the undamaged structure while the nonlinear techniques do not. HOS such as bispectral analysis and bicoherence was used to characterize the second order nonlinearity of the structure due to corrosion, whilst RBF interpolation was applied to a number of signals acquired from a sparse array of sensors, in order to obtain an image of the defect. Compared to standard linear ultrasonic imaging techniques, the robustness of this nonlinear tomography sensing system was experimentally demonstrated: a combination of bicoherence analysis and radial basis function allowed a perfect localization of the pitting corrosion with an error equal to zero.

REFERENCES

[1] F. Ciampa, M. Meo, "Nonlinear elastic imaging using reciprocal time reversal and third order symmetry analysis", *J. Acoust. Soc. Am.*, 131, 4316–4323, (2012).

[2] G. Scarselli, A. Maffezzoli, E. Castorini, A. Taurino, “Vibrational analysis of aerospace composite components for production defects and operating damage detection”, *Proceedings of 9th International Conference on Composite Science and Technology (ICCST9)*, 811-819, (2013).
[3] K.-R. Leonard, E.-V. Malyarenko, M.-K. Hinders, “Ultrasonic Lamb Wave Tomography”, *Inverse Problems*, 18, 1795-1808, (2002).
[4] J.-E. Michaels, T.-E. Michaels, “Guided wave signal processing and image fusion for in situ damage localization in plates”, *Wave Motion*, 44, 482-492, (2007).
[5] A. Croxford, P. Wilcox, B., Drinkwater, G. Konstantinidis, “Strategies for guided-wave structural health monitoring”, *Proc. R. Soc. A*, 463, 2961-2981 (doi:10.1098/rspa.2007.0048), (2007).
[6] J.-E. Michaels, T.-E. Michaels, “Damage Localization in Inhomogeneous Plates Using a Sparse Array of Ultrasonic Transducers”, *AIP Conference Proceedings*, 894, 846-853, (2007).
[7] H. Gao, Y. Shi, J. Rose, “Guided wave tomography on an aircraft wing with leave in place sensors”, *AIP Conf. Proc.*, 760, 1788-1794 (doi:10.1063/1.1916887), (2005).
[8] E. Flynn, M.-D. Todd, P.-D. Wilcox, B.-W. Drinkwater, A. Croxford, “Maximum Likelihood estimation of damage location in guided-wave structural health monitoring”, *Proceedings of The Royal Society A*, (doi: 10.1098/rspa.2011.0095), (2011).
[9] G., Zumpano, M., Meo, “Damage localization using transient non-linear elasticwave spectroscopy on composite structures”, *International Journal of Non-Linear Mechanics*, **43**: 217 – 230, (2008).
[10] M. Meo, G. Zumpano, “Nonlinear elastic wave spectroscopy identification of impact damage on a sandwich plate”, *Composite Structures*, 71: 469–474, (2005).
[11] J., Kyung-Young, “Applications of Nonlinear Ultrasonics to the NDE of Material Degradation”. *IEEE transactions on ultrasonics, ferroelectrics, and frequency control*, 47(3):540-8, (2000).
[12] F. Ciampa, S. Pickering, G. Scarselli, M. Meo, “Nonlinear damage detection in composite structures using bispectral analysis”, *Proc. SPIE. 9064, Health Monitoring of Structural and Biological Systems 2014*, doi: 10.1117/12.2046631, San Diego, (2014).
[13] L. D. Landau, E. M. Lifshitz, [Theory of Elasticity], Chap. III, *Pergamon*, Oxford, (1986).
[14] Y.-C. Kim, E.-J. Powers, “Digital Bispectral Analysis and its Applications to Nonlinear Wave Interactions,” *IEEE Transactions on Plasma Science,* Ps-7, 120-131, (1979).
[15] J. R. Davis, “Corrosion of Aluminium and Aluminium Alloys”, *Edited by J.R. Davis*, 39-40, (1999).
[16] E. Ghali, “Corrosion Resistance of Aluminium and Magnesium Alloys Understanding, Performance, and Testing”, *Series Editor*, 165-166 (2010).